J Mater Sci: Mater Med (2011) 22:151–158
DOI 10.1007/s10856-010-4189-z

Response of human alveolar bone-derived cells to a novel poly(vinylidene fluoride-trifluoroethylene)/barium titanate membrane

L. N. Teixeira · G. E. Crippa · R. Gimenes · M. A. Zaghete · P. T. de Oliveira · A. L. Rosa · M. M. Beloti

Received: 2 September 2010 / Accepted: 10 November 2010 / Published online: 24 November 2010

Abstract This study investigated the response of human alveolar bone-derived cells to a novel poly(vinylidene fluoride-trifluoroethylene)/barium titanate (P(VDF-TrFE)/BT) membrane. Osteoblastic cells were cultured in osteogenic conditions either on P(VDF-TrFE)/BT or polytetrafluoroethylene (PTFE) for up to 14 days. At 7 and 14 days, the mRNA expression of Runt-related transcription factor 2 (RUNX2), Type I collagen (COL I), Osteopontin (OPN), Alkaline phosphatase (ALP), Bone sialoprotein (BSP), and Osteocalcin (OC), key markers of the osteoblastic phenotype, and of Bcl2-associated X protein (Bax), B-cell CLL/lymphoma 2 (Bcl-2), and Survivin (SUR), associated with the control of the apoptotic cell death, was assayed by real-time PCR. In situ ALP activity was qualitatively evaluated by means of Fast red staining. Surface characterization was also qualitatively and quantitatively assayed in terms of topography, roughness, and wettability. Cells grown on P(VDF-TrFE)/BT exhibited a significantly higher mRNA expression for all markers compared to the ones on PTFE, except for Bcl-2, which was not detected for both groups. Additionally, Fast red staining was noticeably stronger in cultures on P(VDF-TrFE)/BT at 7 and 14 days. At micron- and submicron scale, SEM images and roughness analysis revealed that PTFE and P(VDF-TrFE)/BT exhibited a smooth topography and a similar roughness, respectively. PTFE membrane displayed higher contact angles compared with P(VDF-TrFE)/BT, as indicated by wettability assay. The novel P(VDF-TrFE)/BT membrane supports the acquisition of the osteoblastic phenotype in vitro, while up-regulating the expression of apoptotic markers. Further in vivo experiments should be carried out to confirm the capacity of P(VDF-TrFE)/BT membrane in promoting bone formation in guided bone regeneration.

L. N. Teixeira · P. T. de Oliveira · M. M. Beloti (✉)
Department of Morphology, Stomatology and Physiology, School of Dentistry of Ribeirao Preto, University of Sao Paulo, Av. do Cafe, s/n, Ribeirao Preto, SP 14040-904, Brazil
e-mail: mmbeloti@usp.br

G. E. Crippa · A. L. Rosa
Department of Oral and Maxillofacial Surgery and Periodontology, School of Dentistry of Ribeirao Preto, University of Sao Paulo, Ribeirao Preto, SP, Brazil

R. Gimenes · M. A. Zaghete
CMDC, Chemistry Institute of Araraquara, Sao Paulo State University, Sao Paulo, SP, Brazil

1 Introduction

Guided bone regeneration (GBR) has become one of the most widely used techniques for bone regeneration due to its simplicity and efficacy [1, 2]. Such therapy is based on the use of membranes to avoid soft tissue downgrowth into the bone defect, allowing cells with osteogenic potential from medullary spaces and periosteum to populate and regenerate the wounded area [3]. GBR has been applied in maxillofacial surgery to treat alveolar bone defects related to dental implants, to promote alveolar ridge augmentation, and to heal pathological cavities in the jaw bones [4–6].

For GBR applications, membranes should fulfill some prerequisites, including biocompatibility, tissue integration, space maintenance, and clinical manageability [7, 8]. The most frequently used biomaterial in GBR is the expanded polytetrafluoroethylene (e-PTFE), which exhibits an excellent biocompatibility, with no foreign body reaction [9, 10]. Despite that, e-PTFE presents some negative characteristics, such as micromovements and inertness, which may affect the outcomes of GBR [11–13].

Therefore, the development of novel strategies and/or biomaterials is of great interest in this field.

Novel biomaterials can be obtained by the association of different materials [14–18]. In this context, a membrane has recently been developed based on the association of poly(vinylidene fluoride-trifluoroethylene) and barium titanate (P(VDF-TrFE)/BT) [19], aiming to combine the flexibility and easy processability of the polymer and the piezoelectricity of the ceramic [20]. Beloti et al. [21] and Teixeira et al. [22] previously demonstrated that P(VDF-TrFE)/BT composite exhibited a better in vitro biocompatibility compared with PTFE. In the present in vitro study, we hypothesized that such membrane regulates the processes of osteoblastic differentiation and apoptotic cell death at the transcriptional level. To test this hypothesis, we quantitated the mRNA expression levels of key osteoblastic and apoptotic markers by real-time PCR in human alveolar bone-derived cells cultured on P(VDF-TrFE)/BT. Additionally, in situ alkaline phosphatase (ALP) activity was also qualitatively evaluated.

2 Materials and methods

2.1 Membranes and surface characterization

P(VDF-TrFE)/BT membranes were prepared as previously described [19]. A commercially available polytetrafluoroethylene (PTFE) membrane was used as control. All membranes were cut as discs, 12 mm in diameter, and sterilized before using in the cell culture experiments.

Scanning electron microscopy (SEM; LEO-440, LEO Electron Microscopy Ltd, Cambridge, England) was used to assess the surface topography of the membranes. The SEM imaging was carried out using an accelerating voltage of 20 kV. Surface roughness was measured with a profilometer (Mitutoyo SJ201-P, 300 mm accuracy, 0.5 mm/s speed, and five 0.8 mm cut-offs). Three readings (on the center of the membrane, 1 mm to the right and 1 mm to the left) were made in each membrane ($n = 3$). Surface wettability was evaluated using a video-based contact angle meter (CAM 200, KVS Instruments, Helsinki, Finland) by sessile drop method [23]. The contact angle was measured at 0, 5 and 10 min after a drop of the cell culture medium (see composition described below) was placed on the membranes ($n = 3$) at 23.4°C.

2.2 Cell culture

Human alveolar bone fragments (explants) were obtained from healthy donors, using the research protocols approved by the Committee of Ethics in Research of the School of Dentistry of Ribeirao Preto of the University of Sao Paulo. Osteoblastic cells were obtained from these explants by enzymatic digestion using collagenase type II (Gibco-Life Technologies, Grand Island, NY), as described previously [24, 25]. Cells were cultured in α-minimum essential medium (Gibco), supplemented with 10% fetal bovine serum (Gibco), 50 μg/ml gentamicin (Gibco), 0.3 μg/ml fungizone (Gibco), 10^{-7} M dexamethasone (Sigma, St. Louis, MO), 5 μg/ml ascorbic acid (Gibco), and 7 mM β-glycerophosphate (Sigma). Subconfluent cells in primary culture were harvested after treatment with 1 mM ethylenediamine tetraacetic acid (EDTA) (Gibco) and 0.25% trypsin solution (Gibco); then cells were seeded on P(VDF-TrFE)/BT and PTFE membranes placed in 24-well polystyrene plates (Falcon, Franklin Lakes, NJ) at a cell density of either 2×10^4 for Fast red staining [26] or 8×10^4 for real-time PCR [22] cells per well, and subcultured for periods of up to 14 days. During the culture period, cells were incubated at 37°C in a humidified atmosphere of 5% CO_2 and 95% air; the medium was changed every 3 or 4 days.

2.3 Gene expression analysis using real-time PCR

Gene expression of osteoblastic cells cultured on P(VDF-TrFE)/BT and PTFE membranes was assayed by real-time PCR. The genes encoding Runt-related transcription factor 2 (RUNX2), Type I collagen (COL I), Osteopontin (OPN), Alkaline phosphatase (ALP), Bone sialoprotein (BSP), and Osteocalcin (OC), typical markers of the osteoblastic phenotype, as well as the genes encoding BCL2-associated X protein (Bax), B-cell CLL/lymphoma 2 (Bcl-2) and Survivin (SUR), related to the apoptotic process, were evaluated. The primer sequence, melting temperature and predicted amplicon size, were designed using the Primer-Express software (Applied Biosystems, Foster City, CA) and are shown in Table 1.

2.3.1 RNA extraction

At days 7 and 14, total RNA from cells cultured on both membranes was extracted using TRIZOL reagent (Gibco BRL), according to the manufacturer's instructions. The concentration of RNA was determined by optical density at a wavelength of 260 nm, using the GeneQuant (Amersham Biosciences, Piscataway, NJ). The RNA purity was determined from the A260/A280.

2.3.2 Real-time PCR

RNA complementary DNA (cDNA) was synthesized using 1 μg of RNA through a reverse transcription reaction (M-MLV reverse transcriptase, Promega, Madison, WI). Real-time PCR analyses were performed in an ABI

Table 1 Primer sequences and reaction properties

Gene	Primer sense sequence Primer anti-sense sequence	T_M (°C)	bp
RUNX2	TATGGCACTTCGTCAGGATCC AATAGCGTGCTGCCATTCG	83	110
COL I	CCACAAAGAGTCTACATGTCTAGGGTC GTCATCGCACAACACCTTGC	84	114
OPN	AGACACATATGATGGCCGAGG GGCCTTGTATGCACCATTCAA	79	154
ALP	ACGTGGCTAAGAATGTCATC CTGGTAGGCGATGTCCTTA	86	475
BSP	AATCTGTGCCACTCACTGCCTT CCTCTATTTTGACTCTTCGATGCAA	79	201
OC	CAAAGGTGCAGCCTTTGTGTC TCACAGTCCGGATTGAGCTCA	85	150
Bax	GCAAACTGGTGCTCAAGGCC CTCCCGCCACAAAGATGGTC	85	156
Bcl-2	CGCCCTGTGGATGACTGAGTAC CACTTGTGGCCCAGATAGGC	83	201
SUR	GTTAATAAAGCCGTAGGCCCTTGT TTGGAACCTCACCCATAGCC	79	151
β-gus	GAAAATATGTGGTTGGAGAGCTCATT CCGAGTGAAGATCCCCTTTTTA	80	101

The annealing temperature used for all reactions was 60°C

T_M melting temperature, *bp* product size

Prism 7000 Sequence Detection System using the Sybr-Green system (Applied Biosystems). SybrGreen PCR MasterMix (Applied Biosystems), specific primers and 2.5 ng of cDNA were used in each reaction. The standard PCR conditions were 95°C (10 min) and 40 cycles of 94°C (1 min), 56°C (1 min) and 72°C (2 min), followed by the standard denaturation curve. For mRNA analysis, the relative level of gene expression was calculated in reference to both β-gus expression in the sample and its respective control (PTFE membrane) using the cycle threshold (Ct) method [27].

2.4 Detection of in situ ALP activity

At 7 and 14 days, in situ ALP activity was qualitatively evaluated by Fast red staining [28]. Briefly, the medium was removed and the cultures were washed twice with Hanks' balanced salt solution (Sigma) and then incubated with 120 mM Tris buffer (Sigma), pH 8.4, containing 0.9 mM naphthol AS-MX phosphate (Sigma) and 1.8 mM Fast red TR (Sigma). The naphthol AS-MX phosphate was solubilized with *N*,*N* dimethyl formamide (Merck KGaA, Darmstadt, Germany) prior to dilution with the Tris buffer. After 30 min at 37°C, the cultures were washed with sodium phosphate buffer (PB), pH 7.2. Before mounting for microscope observation, the cultures were permeabilized with 0.5% Triton X-100 in PB for 10 min and cell nuclei stained with 300 nM 40,6-diamidino-2-phenylindole, dihydrochloride (DAPI, Molecular Probes) for 5 min. Membranes were placed face up on glass slides, covered with 12-mm-round glass coverslips (Fisher Scientific) and mounted with an antifade kit (Vectashield, Vector Laboratories, Burlingame, CA). The samples were then examined under epifluorescence using a Leica DMLB light microscope (Leica, Bensheim, Germany), with N Plan (X10/0.25, X20/0.40) and HCX PL Fluotar (X40/0.75, X100/1.3) objectives, outfitted with a Leica DC 300F digital camera. Acquired digital images were processed with Adobe Photoshop software (Adobe Systems).

2.5 Statistical analysis

Roughness and wettability were carried out in triplicate ($n = 3$) and data were analyzed using either Student's *t* test or analysis of variance (two-way ANOVA), followed by Tukey's post-hoc test when appropriate. Real-time PCR results described below are representative of 2 sets of cultures and was carried out in quintuplicate ($n = 5$). Data were statistically analyzed using Mann–Whitney *U* test for non-paired examination followed by Bonferroni's correction. The significant level was established at $P \leq 0.05$.

3 Results

P(VDF-TrFE)/BT and PTFE membranes showed similar features in terms of surface topography, exhibiting an apparent smooth surface, as observed by SEM analysis (Fig. 1). The surface roughness was statistically similar for both membranes at micron- and submicron scale (Student's *t* test, $P = 0.574$; Fig. 2a). Static contact angles were affected by membrane composition and time (two-way ANOVA, $P = 0.001$; Fig. 2b). PTFE exhibited higher values of static contact angles compared with the ones observed in P(VDF-TrFE)/BT. The decrease of contact angles was affected by time (0 min > 5 min = 10 min).

Real-time PCR analysis revealed a significantly higher expression of RUNX2, COL I, OPN, ALP, BSP, and OC in osteoblastic cultures grown on P(VDF-TrFE)/BT compared with PTFE at 7 and 14 days ($P = 0.032$, for all genes and both time points; Fig. 3). The apoptotic-related genes Bax and SUR were also up-regulated in cells cultured on P(VDF-TrFE)/BT at days 7 and 14 ($P = 0.032$, for all genes and both time points; Fig. 4). Although Bcl-2 was expressed in cells cultured on polystyrene, Bcl-2 mRNA was detected in very low levels as revealed by its high Ct value (>33) on both membranes and the calculation of gene

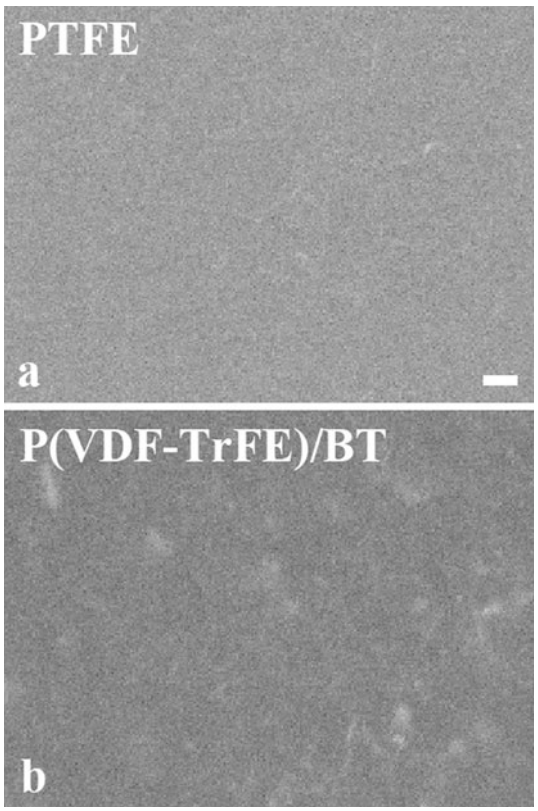

Fig. 1 High resolution SEM imaging of PTFE (**a**) and P(VDF-TrFE)/BT (**b**). At micron-scale both membranes exhibited a smooth surface. *Scale bar* for **a**–**b** = 6 μm

expression may not represent the biological event. Because of this, results of Bcl-2 were not shown.

Epifluorescence revealed a higher cell population density with a stronger Fast red staining for cultures on P(VDF-TrFE)/BT compared with the ones on PTFE at 7 and 14 days (Fig. 5, compare b with a and d with c).

4 Discussion

The results of this study showed that the expression of mRNA levels of key osteoblastic and apoptotic markers was significantly enhanced in human alveolar bone-derived cell cultures grown on P(VDF-TrFE)/BT membrane compared with PTFE. In addition, in situ ALP activity was noticeably higher on P(VDF-TrFE)/BT, as judged by stronger Fast red staining. These findings indicate that P(VDF-TrFE)/BT membrane supports the acquisition of the osteoblastic phenotype both at the transcriptional and protein levels in vitro, while up-regulating genes associated with the apoptotic cell death program.

Among several transcription factors involved in the early stages of bone formation, RUNX2 has been recognized as the main factor controlling osteoblast commitment and differentiation [29, 30]. During the process of osteoblastic differentiation, matrix proteins including COL I, OPN, BSP, and OC are synthesized and secreted in temporally and spatially characteristic patterns, and therefore represent important parameters to be assayed [31]. In the context of GBR, bone and intrabony defects covered with PTFE membranes display a greater expression of RUNX2, COL I, OPN, BSP, and OC compared with non-covered sites [32, 33]. Our in vitro results showed that osteoblastic cells cultured on P(VDF-TrFE)/BT exhibited a markedly higher expression of RUNX2, COL I, OPN, BSP, and OC compared with those on PTFE. These findings suggest that P(VDF-TrFE)/BT may represent an additional stimulus for bone regeneration when the use of membranes is indicated.

During the course of collagen matrix mineralization, the presence of inorganic phosphate in the extracellular milieu is essential to ensure the occurrence of hydroxyapatite nucleation and growth [31, 34]. The supplying of inorganic phosphate is provided by ALP enzyme [35]. Cells cultured on P(VDF-TrFE)/BT membrane exhibited a higher expression of ALP gene associated with an intense in situ ALP activity, indicating that the interaction of osteoblastic cells with this novel composite creates favorable biochemical conditions that ultimately support matrix mineralization. Indeed, bone-like mineralized nodules have only been observed in osteoblastic cultures grown on P(VDF-TrFE)/BT [21].

Some characteristics of the substrate could account for the observed differences in the gene expression profiling and ALP activity between osteoblastic cell cultures grown on P(VDF-TrFE)/BT and PTFE. Indeed, it has been

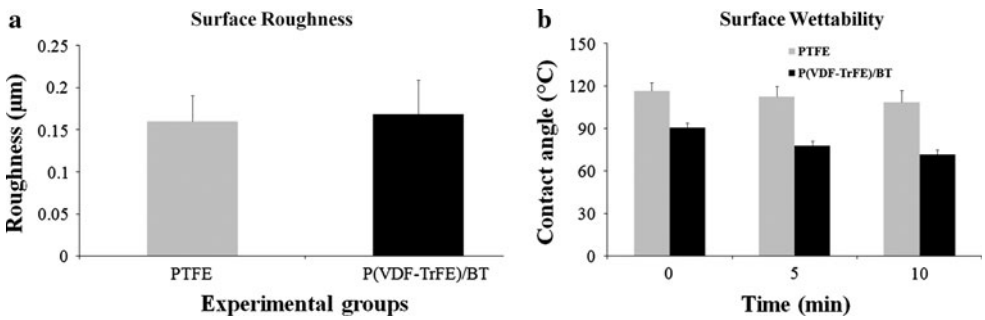

Fig. 2 Surface roughness (**a**) and wettability (**b**) of PTFE and P(VDF-TrFE)/BT membranes. Data are reported as mean ± SD

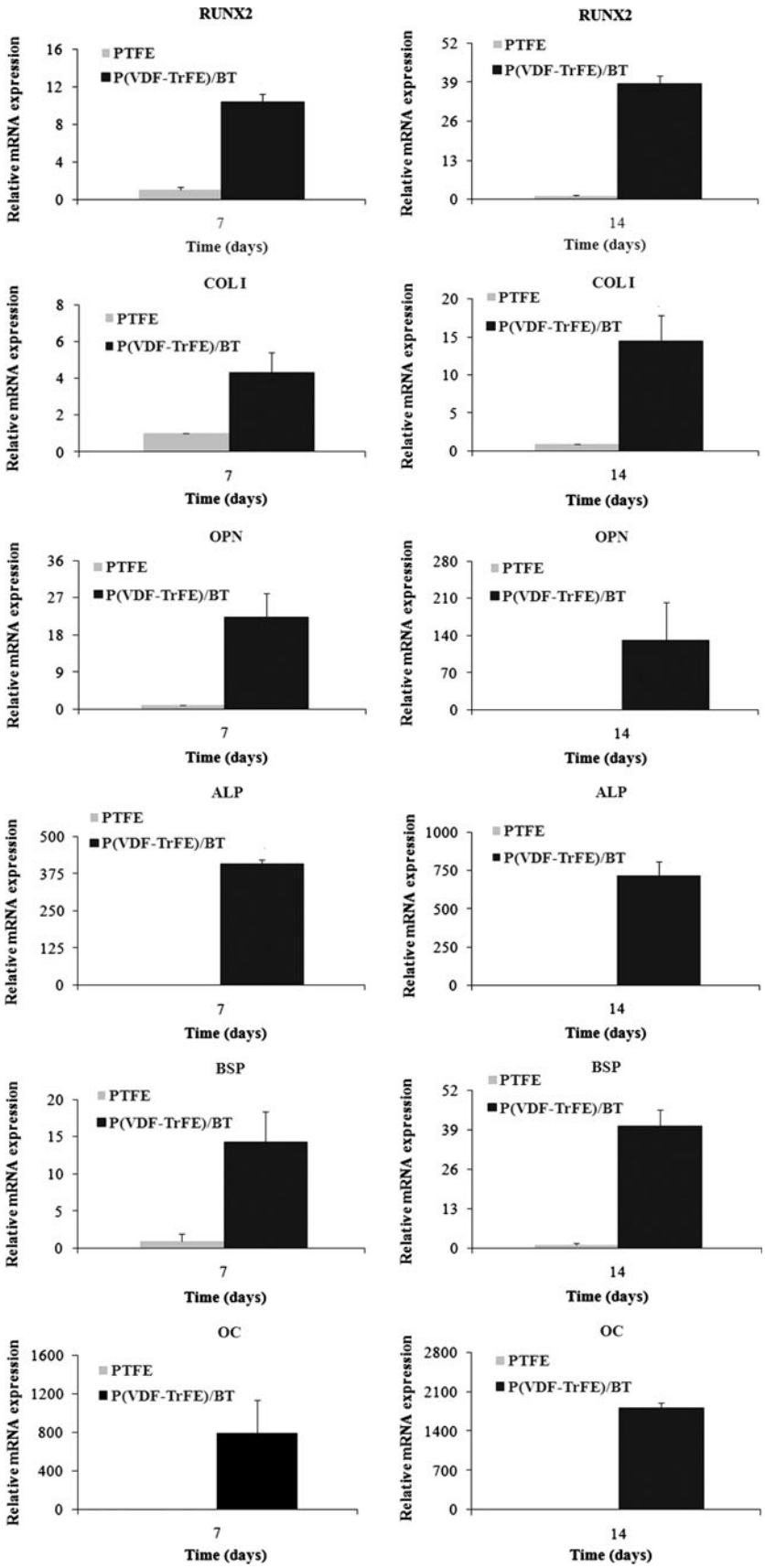

Fig. 3 RUNX2, COL I, OPN, ALP, BSP, and OC mRNA expression in human alveolar bone-derived cells cultured on PTFE and P(VDF-TrFE)/BT at days 7 and 14 by means of real-time PCR. Data were calculated as the relative expression of the target mRNA normalized to β-gus and to PTFE (calibrator) and are reported as mean $\pm$ SD

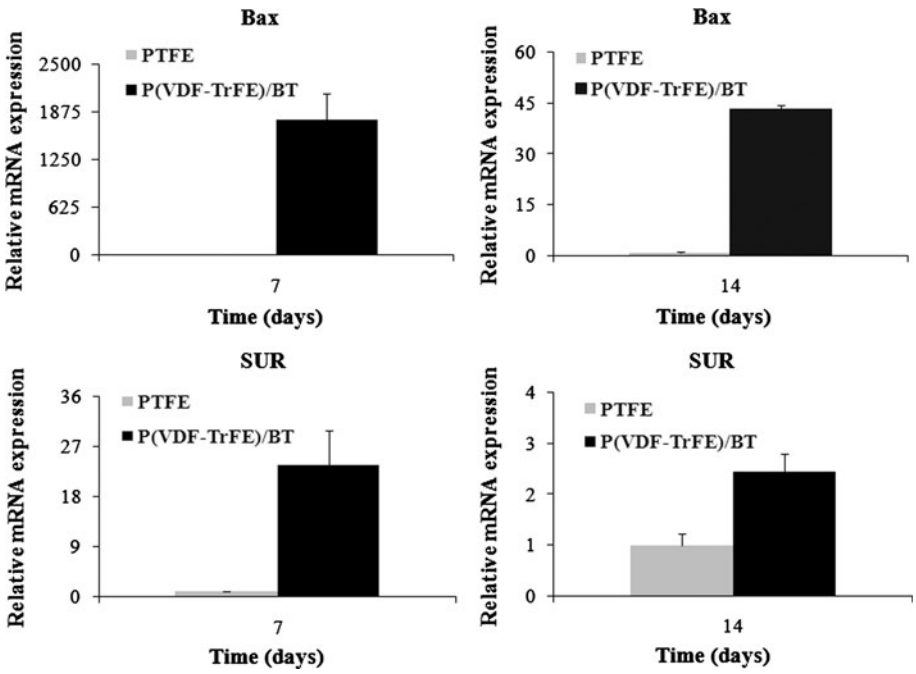

Fig. 4 Bax and SUR mRNA expression in human alveolar bone-derived cells cultured on PTFE and P(VDF-TrFE)/BT at days 7 and 14 by means of real-time PCR. Data were calculated as the relative expression of the target mRNA normalized to β-gus and to PTFE (calibrator) and are reported as mean ± SD

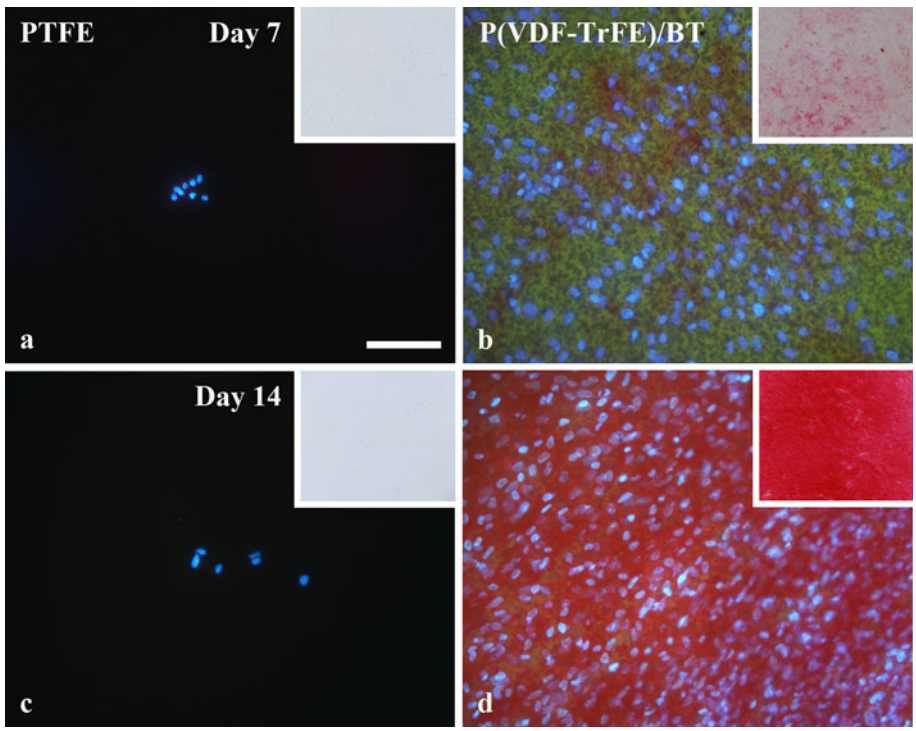

Fig. 5 Epifluorescence of in situ ALP activity of human alveolar bone-derived cells cultured on PTFE (**a**, **c**) and P(VDF-TrFE)/BT (**b**, **d**) at days 7 (**a**, **b**) and 14 (**c**, **d**). Fast red (*red fluorescence*) and DAPI DNA staining (*blue fluorescence*) revealed, respectively, larger areas of ALP activity and a higher cell density for cultures grown on P(VDF-TrFE)/BT compared with PTFE. Differences between both groups in terms of ALP activity were also clearly noticed at the macroscopic level (*insets*). *Scale bar* for **a**–**d** = 100 μm; for *insets* = 4.2 mm. (Color figure online)

demonstrated that surface topography, chemistry, energy/wettability may affect protein adsorption and the progression of the osteogenic phenotype in vitro [36–40]. Although the surface roughness was similar for both membranes at micron- and submicron scale, P(VDF-TrFE)/BT exhibited a more wettable surface than PTFE, as indicated by the contact angle measurement. Wettability has been reported as an essential physicochemical property of biomaterials that might control protein adsorption and cell behavior [41, 42]. Actually, an increase in surface wettability leads to a higher cell attachment, proliferation and protein synthesis [43]. Therefore, the lower mRNA expression levels and in situ ALP activity observed in cultures grown on PTFE could thus be due to a low protein binding capacity and decreased wettability, as demonstrated elsewhere [44, 45].

During bone formation and regeneration, osteoblasts undergo an orderly developmental progression that ultimately ends in apoptosis [46]. Several genes are involved in the apoptotic cell death, including Bcl-2, Bax, and SUR. The balance between Bcl-2 and Bax genes determines the cell fate. If Bax is overexpressed, the cell undergoes apoptosis. Conversely, if Bcl-2 expression prevails, the cell is protected against apoptosis [47, 48]. Survivin is a regulatory protein that controls apoptosis by inhibiting caspase activity [49, 50]. In the present study, a higher expression of the apoptotic genes Bax and SUR was observed in cultures grown on P(VDF-TrFE)/BT compared with PTFE at days 7 and 14. One possible explanation for such finding could rely on the more advanced stages in the osteoblastic differentiation sequence for cells grown on P(VDF-TrFE)/BT substrate, as judged by the up-regulation of the bone markers used.

In conclusion, we demonstrated that a novel membrane of the P(VDF-TrFE)/BT composite supports the up-regulation of bone and apoptotic markers and ALP activity in human alveolar bone-derived cell cultures. Therefore, the use of P(VDF-TrFE)/BT in GBR could likely promote bone matrix formation along and adjacently to the membrane, a concept that should be taken into consideration especially for larger bone defects (critical-sized defects). Further in vivo studies using animal models for GBR should be carried out to test whether the process of bone repair would be benefit from the use of P(VDF-TrFE)/BT.

Acknowledgments The authors thank The State of Sao Paulo Research Foundation (FAPESP, Brazil) and The National Council of Scientific and Technological Development (CNPq) for the financial support and Roger Rodrigo Fernandes for technical assistance. The authors would also to thank Felippe José Pavinatto and Ana Paula Macedo for helpful assistance with wettability and roughness assay, respectively. Lucas Novaes Teixeira was the recipient of a Masters scholarship from FAPESP. The authors declare that they have no conflict of interest.

References

1. Hämmerle CH, Schmid J, Lang NP, et al. Temporal dynamics of healing in rabbit cranial defects using guided bone regeneration. J Oral Maxillofac Surg. 1995;53(2):167–74.
2. Piattelli A, Scarano A, Russo P, et al. Evaluation of guided bone regeneration in rabbit tibia using bioresorbable and non-resorbable membranes. Biomaterials. 1996;17(8):791–6.
3. Dahlin C, Linde A, Gottlow J, et al. Healing of bone defects by guided tissue regeneration. Plast Reconstr Surg. 1988;81(5):672–6.
4. Dahlin C, Gottlow J, Linde A, et al. Healing of maxillary and mandibular bone defects using a membrane technique. An experimental study in monkeys. Scand J Plast Reconstr Surg Hand Surg. 1990;24(1):13–9.
5. Seibert J, Nyman S. Localized ridge augmentation in dogs: a pilot study using membranes and hydroxyapatite. J Periodontol. 1990;61(3):157–65.
6. Hämmerle CH, Karring T. Guided bone regeneration at oral implant sites 2000. Periodontology. 1998;17:151–75.
7. Scantlebury TV. 1982–1992: A decade of technology development for guided tissue regeneration. J Periodontol. 1993;64(11 Suppl):1129–37.
8. Laurell L, Gottlow J. Guided tissue regeneration update. Int Dent J. 1998;48(4):386–98.
9. Dahlin C. Scientific background of guided bone regeneration. In: Buser D, Dahlin C, Schenk RK, editors. Guided bone regeneration in implant dentistry. Chicago: Quintessence Publishing; 1994. p. 31–48.
10. Schenk RK, Buser D, Hardwick WR, et al. Healing pattern of bone regeneration in membrane-protected defects: a histologic study in the canine mandible. Int J Oral Maxillofac Implants. 1994;9(1):13–29.
11. Nyman S. Bone regeneration using the principle of guided tissue regeneration. J Clin Periodontol. 1991;18(6):494–8.
12. Sandberg E, Dahlin C, Linde A. Bone regeneration by the osteopromotion technique using bioabsorbable membranes: an experimental study in rats. J Oral Maxillofac Surg. 1993;51(10):1106–14.
13. Dahlin C, Simion M, Nanmark U, et al. Histological morphology of the e-PTFE/tissue interface in humans subjected to guided bone regeneration in conjunction with oral implant treatment. Clin Oral Implants Res. 1998;9(2):100–6.
14. Liao S, Watari F, Zhu Y, et al. The degradation of the three layered nano-carbonated hydroxyapatite/collagen/PLGA composite membrane in vitro. Dent Mater. 2007;23(9):1120–8.
15. Sui G, Yang X, Mei F, et al. Poly-L-lactic acid/hydroxyapatite hybrid membrane for bone tissue regeneration. J Biomed Mater Res A. 2007;82(2):445–54.
16. Teng SH, Lee EJ, Wang P, et al. Three-layered membranes of collagen/hydroxyapatite and chitosan for guided bone regeneration. J Biomed Mater Res B Appl Biomater. 2008;87(1):132–8.
17. Tokuda S, Obata A, Kasuga T. Preparation of poly(lactic acid)/siloxane/calcium carbonate composite membranes with antibacterial activity. Acta Biomater. 2009;5(4):1163–8.
18. Park JK, Yeom J, Oh EJ, et al. Guided bone regeneration by poly(lactic-co-glycolic acid) grafted hyaluronic acid bi-layer films for periodontal barrier applications. Acta Biomater. 2009;5(9):3394–403.
19. Gimenes R, Zaghete MA, Bertolini M, et al. Composites PVDF-TrFE/BT used as bioactive membranes for enhancing bone regeneration. Proc SPIE. 2004;5385:539–47.
20. Dias CJ, Das-Gupta DK. Poling behaviour of ceramic/polymer ferroelectric composites. Ferroelectrics. 1994;157(1):405–10.
21. Beloti MM, de Oliveira PT, Gimenes R, et al. In vitro biocompatibility of a novel membrane of the composite poly(vinylidene-trifluoroethylene)/barium titanate. J Biomed Mater Res A. 2006;79(2):282–8.
22. Teixeira LN, Crippa GE, Trabuco AC, et al. In vitro biocompatibility of poly(vinylidene fluoride-trifluoroethylene)/barium titanate composite using cultures of human periodontal ligament fibroblasts and keratinocytes. Acta Biomater. 2010;6(3):979–89.
23. Adamson AW, Gast AP. The solid–liquid interface-contact angle. In: Adamson AW, Gast AP, editors. Physical chemistry of surfaces. New York: Wiley; 1997. p. 347–89.
24. Beloti MM, Tambasco De Oliveira P, Perri De Carvalho PS, et al. Seeding osteoblastic cells into a macroporous biodegradable CaP/PLGA scaffold by a centrifugal force. J Biomater Appl. 2009;23(6):481–95.
25. De Assis AF, Beloti MM, Crippa GE, et al. Development of the osteoblastic phenotype in human alveolar bone-derived cells grown on a collagen type I-coated titanium surface. Clin Oral Implants Res. 2009;20(3):240–6.

26. Moura J, Teixeira LN, Ravagnani C, et al. In vitro osteogenesis on a highly bioactive glass-ceramic (biosilicate). J Biomed Mater Res A. 2007;82(3):545–57.
27. Livak KJ, Schmittgen TD. Analysis of relative gene expression data using real-time quantitative PCR and the 2(−Delta Delta C(T)) Method. Methods. 2001;25(4):402–8.
28. Majors AK, Boehm CA, Nitto H, et al. Characterization of human bone marrow stromal cells with respect to osteoblastic differentiation. J Orthop Res. 1997;15(4):546–57.
29. Lian JB, Stein GS. Runx2/Cbfa1: a multifunctional regulator of bone formation. Curr Pharm Des. 2003;9(32):2677–85.
30. Marie PJ. Transcription factors controlling osteoblastogenesis. Arch Biochem Biophys. 2008;473(2):98–105.
31. Beck GR Jr. Inorganic phosphate as a signaling molecule in osteoblast differentiation. J Cell Biochem. 2003;90(2):234–43.
32. Tanaka S, Matsuzaka K, Sato D, et al. Characteristics of newly formed bone during guided bone regeneration: analysis of cbfa-1, osteocalcin, and VEGF expression. J Oral Implantol. 2007;33(6): 321–6.
33. Lima LL, Gonçalves PF, Sallum EA, et al. Guided tissue regeneration may modulate gene expression in periodontal intrabony defects: a human study. J Periodontal Res. 2008;43(4): 459–64.
34. Bellows CG, Heersche JN, Aubin JE. Inorganic phosphate added exogenously or released from beta-glycerophosphate initiates mineralization of osteoid nodules in vitro. Bone Miner. 1992; 17(1):15–29.
35. Sugawara Y, Suzuki K, Koshikawa M, et al. Necessity of enzymatic activity of alkaline phosphatase for mineralization of osteoblastic cells. Jpn J Pharmacol. 2002;88(3):262–9.
36. Schwartz Z, Boyan BD. Underlying mechanisms at the bone–biomaterial interface. J Cell Biochem. 1994;56(3):340–7.
37. Schwartz Z, Kieswetter K, Dean DD, et al. Underlying mechanisms at the bone–surface interface during regeneration. J Periodontal Res. 1997;32(1 Pt 2):166–71.
38. De Oliveira PT, Zalzal SF, Beloti MM, et al. Enhancement of in vitro osteogenesis on titanium by chemically produced nanotopography. J Biomed Mater Res A. 2007;80(3):554–64.
39. Liu X, Lim JY, Donahue HJ, et al. Influence of substratum surface chemistry/energy and topography on the human fetal osteoblastic cell line hFOB 1.19: phenotypic and genotypic responses observed in vitro. Biomaterials. 2007;28(31):4535–50.
40. Rosa AL, Crippa GE, de Oliveira PT, et al. Human alveolar bone cell proliferation, expression of osteoblastic phenotype, and matrix mineralization on porous titanium produced by powder metallurgy. Clin Oral Implants Res. 2009;20(5):472–81.
41. Anselme K. Osteoblast adhesion on biomaterials. Biomaterials. 2000;21(7):667–81.
42. Wei J, Igarashi T, Okumori N, et al. Influence of surface wettability on competitive protein adsorption and initial attachment of osteoblasts. Biomed Mater. 2009;4(4):045002 (7 pp).
43. Thian ES, Ahmad Z, Huang J, et al. The role of surface wettability and surface charge of electrosprayed nanoapatites on the behaviour of osteoblasts. Acta Biomater. 2010;6(3):750–5.
44. Brunette DM. The effects of implant surface topography on the behavior of cells. Int J Oral Maxillofac Implants. 1988;3(4): 231–46.
45. Salonen JI, Persson GR. Migration of epithelial cells on materials used in guided tissue regeneration. J Periodontal Res. 1990;25(4): 215–21.
46. Hock JM, Krishnan V, Onyia JE, et al. Osteoblast apoptosis and bone turnover. J Bone Miner Res. 2001;16(6):975–84.
47. Oltvai ZN, Milliman CL, Korsmeyer SJ. Bcl-2 heterodimerizes in vivo with a conserved homolog, Bax, that accelerates programmed cell death. Cell. 1993;74(4):609–19.
48. Yang E, Zha J, Jockel J, et al. Bad, a heterodimeric partner for Bcl-XL and Bcl-2, displaces Bax and promotes cell death. Cell. 1995;80(2):285–91.
49. Deveraux QL, Stennicke HR, Salvesen GS, et al. Endogenous inhibitors of caspases. J Clin Immunol. 1999;19(6):388–98.
50. Salvesen GS, Duckett CS. IAP proteins: blocking the road to death's door. Nat Rev Mol Cell Biol. 2002;3(6):401–10.